





Original Research Article

Performance and Stability Evaluation of Low-Cost Inorganic Methyl Ammonium Lead Iodide (CH₃NH₃PbI₃) Perovskite Solar Cells Enhanced with Natural Dyes from Cashew and Mango Leaves

Ejeka Joshua Chukwuemeka^{1,2} , Nwokoye Anthony Osita², Anyanor Oliver Odira², Udeze Chinwe Uchekchukwu^{2,3} , Jeroh Diemiruaye Mimi² , Imosobomeh Lucky Ikhioya^{4,5*} 

¹ Department of Industrial Physics, Abia State University, Uturu, Abia State, Nigeria

² Department of Physics and Industrial Physics, Nnamdi Azikiwe University Awka, Anambra State, Nigeria

³ Department of Mechanical, Electrical and Manufacturing Engineering, Loughborough University, London, United Kingdom

⁴ Department of Physics and Astronomy, University of Nigeria, Nsukka, Nigeria

⁵ National Centre for Physics, Quaid-i-Azam University Campus, Islamabad, Pakistan

ARTICLE INFO

Article history

Submitted: 14 July 2023

Revised: 19 September 2023

Accepted: 15 October 2023

Available online: 18 October 2023

Manuscript ID: [AJCA-2307-1384](#)

Checked for Plagiarism: [Yes](#)

Language editor:

[Dr. Fatimah Ramezani](#)

Editor who approved publication:

[Dr. Hoda Hamidi](#)

DOI: [10.48309/ajca.2024.406961.1384](https://doi.org/10.48309/ajca.2024.406961.1384)

KEYWORDS

Perovskite solar cells

Cashew dye

Mango dye

Aqueous extraction

Bandgap

ABSTRACT

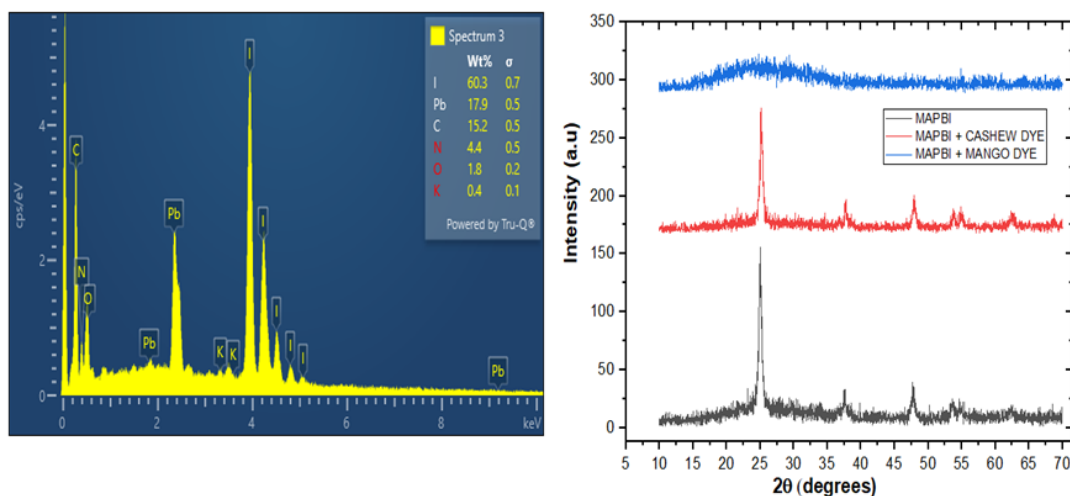
The primary hindrance to widespread solar energy adoption has been the high initial cost of technology. Traditional silicon solar cells, while efficient, are costly. Perovskite solar cells face three key challenges: instability under various conditions, environmental toxicity from synthetic additives and solvents, and long-term reliability concerns. To address this, we are exploring perovskite solar cells (PSCs) for their potential cost-effectiveness by enhancing PSC performance and stability using natural dyes extracted from cashew and mango leaves, offering an eco-friendly solution to toxic additives. The band gaps of the pristine device and those incorporating cashew dye and mango dye were measured at 1.59 eV, 1.70 eV, and 2.52 eV, respectively. The samples that were prepared were confirmed to be polycrystalline in nature through XRD analysis. The SEM analysis offered valuable insights into the morphological characteristics of the perovskite films before and after dye treatment, each sample exhibiting unique attributes. The perovskite solar cell with mango dye had a PCE of 0.0297% and an improved FF of 0.571. After 1032 hours the optical properties of the samples were monitored under room temperature and conditions to assess their stability. The dye-treated samples demonstrated favorable absorption, increased transmittance, and decreased reflectance, making them a viable option for optoelectronic and tandem solar cell applications. The band gap values of the pristine device and devices with cashew and mango dyes were 2.90 eV, 2.15 eV, and 2.17 eV, respectively.

* Corresponding author: Ikhioya, Imosobomeh Lucky

✉ E-mail: imosobomeh.ikhioya@unn.edu.ng

© 2024 by SPC (Sami Publishing Company)

GRAPHICAL ABSTRACT



Introduction

Combustion of fossil fuels has caused adverse environmental impacts, such as increased emissions, global warming, rising sea levels, biodiversity loss, food scarcity, and deteriorating health conditions [1,2], prompting the need for alternative energy sources. Among these alternatives, solar energy has emerged as a promising and sustainable solution. Solar cells have improved in recent decades, leading to better energy conversion and lower costs [3-5]. Solar energy is widely accepted as an alternative to non-renewable resources, with a large increase in capacity worldwide [6]. Power conversion efficiency has increased tenfold since the early days of crystalline silicon solar cells, which had 4% efficiency. There have been three generations of solar cell technology, each with unique materials and fabrication techniques [6-8]. The first generation of solar cells, based on silicon wafers, has achieved high power conversion efficiencies approaching the theoretical limits of 33%. The high cost of silicon cells has led to the search for other methods. Thin-film solar cells are more cost-effective and require less material than silicon-based cells. GaAs, CdTe, CIGS, and amorphous silicon have achieved impressive results, such as a peak

efficiency of 47.1%. Complex preparation techniques and potential environmental threats limit the adoption of thin-film solar cells [7]. The third generation of solar cells is composed of nanocrystals and nanoporous materials. Perovskite, Dye-sensitized and Organic Photovoltaics are all part of this generation of solar cells. PSCs are attractive due to their low-cost fabrication process, tunable band gaps, and efficient and light-active structures [8-16].

PSCs include mixed organic-inorganic halide materials, typically with the general chemical formula ABX_3 . Metal cations A and B, with A being larger, combine with +6 ionic valences, while X is an electronegative anion with -2 ionic valence. Perovskite materials come in various forms and can be processed by spray pyrolysis, dip coating, etc. In a typical PSC structure, a perovskite active layer is sandwiched between electron and hole transport layers. The perovskite layer absorbs light producing excitons, which are separated into free charges and used to generate electrical current. Research has sought to improve PSC performance by increasing light absorption and charge transport [9,10,17]. DSSCs usually use organic dyes to absorb light, but PSCs play different dye roles due to their inherent light absorption properties.

Expensive and toxic synthetic dyes which require complex manufacturing procedures have been used to improve the efficiency and stability of PSCs [11-17]. Guanidinium (GA) and 2-(4-methoxyphenyl) ethylamine hydrobromide ($\text{CH}_3\text{O-PEABr}$) are utilized to reduce trap inducement, enhance low trap activity, and smooth the perovskite surface [18].

This work incorporates the use of low-cost natural dyes from plants to improve power conversion efficiency, stability, and charge transport. Natural dyes can be extracted from plants using facile techniques including aqueous, solvents extraction, maceration, or ultrasound [19,20]. These plant-based dyes can be modified chemically for improved electron injection and charge transport [21-28].

Natural dyes from plants are promising for optoelectronic devices due to their availability, cost-effectiveness, eco-friendliness, and wide range of absorption. Cashew and mango leaf extracts are cost-effective and have favorable optoelectronic features [29]. Cashew leaves have a special blend of natural dyes that absorb light from a wide range of wavelengths. This property opens the paths for enhanced light harvesting, especially in indoor and low-light conditions. Natural dyes are stable and safe, which contributes to the PSCs' performance and compatibility [30-35]. Mango leaves have good transmittance levels, making them useful for photoelectric conversion. Mango leaves contain tannin, anthocyanin, and carotenoids.

This study entails the novel incorporation of low-cost natural dyes sourced from cashew (*Anacardium occidentale*) and mango (*Mangifera indica*) leaves, abundantly available in numerous tropical regions. The goal is to exploit these natural dyes as efficacious additives to improve the performance and stability of Methyl Ammonium Lead Iodide (MAPbI₃) perovskite solar cells. The active MAPbI₃ were deposited on a pH-optimized copper-doped nickel oxide hole transport layer through rapid thermal processing

at a controlled temperature of 70 °C using a Doctor Balde technique. For a comprehensive evaluation of the perovskite solar cells (PSC), Scanning Electron Microscopy (SEM), X-ray Diffraction (XRD), Solar simulation and Energy Dispersive X-ray spectroscopy (EDX/EDS) analyses were utilized to scrutinize the structural attributes, surface morphology, crystalline, and electronic properties of the PSC. Moreover, to gain insights into the optical stability characteristics, we conducted a comparative investigation between the untreated (pristine) and dye-enhanced PSC. This comparative analysis was performed using the UV spectroscopy after subjecting the solar cells to an extensive 1032-hour testing period.

This research endeavor not only explores the viability of natural dye additives, but also contributes to advancing the field of perovskite solar cell technology, offering potential solutions for harnessing sustainable and cost-effective renewable energy sources.

Materials and Methods

Materials used in this study include Deionized and distilled water (H_2O), dimethyl formamide (DMF), isopropanol, Lead nitrate $\text{Pb}(\text{NO}_3)_2$, potassium iodide PbI_2 , Hydroiodic acid, Methylamine purchased from Sigma-Aldrich Chemicals, Copper sulfate (CuS), Sodium Hydroxide (NaOH) and Hexahydrate nickel chloride ($\text{NiCl}_2 \cdot 6\text{H}_2\text{O}$), Acetone, Cashew leaves (*Anacardium occidentale*), Fluorine-doped Tin Oxide (FTO) conducting glass substrates, PTFE filter, Ultrasonicator (JL-60DTH), magnetic stirrer, spatula, temperature-controlled hotplate, aluminum foil, sieve, detergent, and blender.

Extraction of Natural Dyes

The samples of Cashew (*Anacardium occidentale*) and Mango (*Mangifera indica*) leaves used were harvested from farms in the southeastern part of Nigeria. The leaves were properly washed with water to remove dust and

dirt. The samples were further rinsed with distilled water and acetone to ensure further decontamination of the samples and dried for seven days under room temperature conditions to avoid loss of chlorophyll due to exposure to sunlight. 12 g of each blended sample was measured and dissolved in 150 mL of acetone for 72 h at room temperature in a conical flask and covered with aluminum foil (to prevent evaporation of the solvent), the solution was agitated at 6hrs intervals to ensure adequate extraction of the chlorophyll [36], and then the natural dyes were extracted by double filtration technique using filter paper to extract the dye. The extracted dyes were subjected to a chemical bath process at 50 °C to remove the acetone used in the extraction process thereby retaining the dye.

Substrate Treatment

The fluorine-doped Tin Oxide (FTO) conducting glass slides were cleaned using an Ultrasonicator bath at 50 °C. The glass slides were initially cleaned with acetone solution and were ultrasonicated for 30 min. Next, the ultrasonicated glass slides with acetone were cleaned with deionized water and ultra-sonicated for another 30 min. Finally, the glass slides were rinsed with deionized water and dried in an oven at 60 °C before being used for deposition. The conductive side of the FTO substrate was determined using a digital multimeter (DT-830D).

Synthesis of Lead-Iodide (PbI₂)

PbI₂ was synthesized by reacting 5g of lead-nitrate Pb(NO₃)₂ dissolved in 25 mL of deionized water in one beaker and stirred until uniform solution nitrate of Pb(NO₃)₂ was observed. 5 g of potassium iodide was dissolved in 25 mL of deionized water in another beaker and stirred continuously until a uniform solution of potassium iodide (PbI₂) was formed. Both solutions were mixed and stirred for a further 20

min using a magnetic stirrer. A yellow precipitate of PbI₂ and a transparent liquid of PbNO₃ were obtained and a simple filtration technique was used to separate the PbI₂ particles from the transparent PbNO₃ liquid. The yellow precipitate PbI₂ particles left on the filter paper were oven dried.

Synthesis of Methyl Ammonium Iodide (CH₃NH₃I)

CH₃NH₃I was synthesized by reacting 30.0 mL of methyl ammine (CH₃NH₂) and 30.0 mL of hydroiodic acid (HI) in a water bath. The perovskite precursor solution was prepared by reacting of 140 mg of the as-prepared PbI₂ with 240 mg of CH₃NH₃I in 1.0 mL of DMF. The mixture was stirred for 1 h at 60 °C to obtain a homogenous solution of CH₃NH₃PbI₃.

Synthesis of Copper Doped Nickel Oxide (Cu: NiO₂)

The pH-optimized Cu: NiO₂ for the perovskite device hole transporting layer was synthesized by reacting CuS, NaOH, and NiCl₂·6H₂O as the copper, oxygen, and nickel sources, respectively. 0.497 g of CuS, 1.3613 g of NiCl, and 0.4 g of NiCl₂·6H₂O were dissolved in 100 mL of distilled water at room temperature for 45 min. 20 mL of each precursor was added to a fresh beaker to form the electrolyte bath. The pH of the prepared electrolyte was 2.3 [37-41].

Deposition of the Copper doped Nickel Oxide (Cu: NiO₂) as HTL on FTO

The Cu: NiO₂ was deposited on the cleaned FTO using the electrodeposition method [42-46]. The electrodeposition parameters were set at a DC voltage of 10V, deposition time of 60 s and room temperature; a three-electrode electrodeposition setup was employed. The FTO substrate was connected to the negative terminal (cathode), the carbon electrode connected to the positive terminal (anode), and a reference silver electrode, all immersed in the electrolyte bath.

MAPbI₃ Deposition

The one-step rapid thermal processing (RTP) and Dr. Blade (blade-coating) method were used in the deposition of the as-prepared MAPbI₃. The substrate was pre-heated to a temperature of 70 °C for 10 min, and then three drops of the as-prepared MAPbI₃ ink were dropped on the substrate while the glass rod blade spread the perovskite through the active area surface of the substrate. The expected color change in the perovskite (from yellow to black) was observed immediately after the blade rolled through the surface, which confirms the rapid crystallization of the perovskite. The sample was allowed to anneal to 110 °C for 20 min to aid the removal of DMF and IPA used in the perovskite synthesis [47,48].

Deposition of the Dyes

The cashew and mango dye extracts were added to the deposited perovskites, respectively, using the Dr. Blade technique. 0.1 mL of the prepared dyes were deposited on top of each MAPbI₃ substrate, 3 min after the roller blade passed through the perovskite then was annealed at 110 °C for further 17 min.

Counter Electrode Preparation

The counter electrode was made from another FTO conductive glass. A digital multimeter (DT-830D) was used to check for the conductive face of the glass. A pencil made of lead was used to coat the conductive face of the glass substrate. No masking tape was required for the two parallel edge of this electrode, and thus the whole surface was coated. A counter carbon electrode was deposited on an FTO which was used to coat the prepared MAPbI₃ to aid electrical contact for the subsequent I-V measurements.

Results and Discussion

Optical Characterization

The optical characterization of the as-deposited MAPbI₃ treated with cashew and mango dyes

was carried out, using the UV-Vis spectrophotometer for the wavelength range of 200-1200 nm. The perovskites stability was investigated after 1032 hours by repeating the optical test. Figure 1A displays the absorption spectra of all synthesized perovskites solar cells. Both the pristine and natural dye-treated MAPbI₃ thin film absorption spectra exhibit a similar absorption profile. The absorption spectra reveal that the films grown under the same parametric conditions at room temperature are more intense in the ultraviolet region with peaks at 0.21, 0.12, and 0.09 for mango dye, cashew dye, and pristine, respectively. The absorbance is seen to gradually decrease towards the visible and near-infrared regions [24]. However, after 1032 hours, the absorbance plot shows that the pristine MAPbI₃ retained its absorptivity having the highest absorbance while other samples had decreased absorbance except for MAPbI₃ containing cashew dye. According to Figure 1B, the least transmittance is observed in Mango Dye treated MAPbI₃ which decreased from about 78% in the NIR to 62% in the UV region, while the pristine MAPbI₃ had the highest transmittance of 82% which was relatively constant from the UV to the NIR. After 1032 hours, the pristine and cashew dye device showed reduced transmittance from 76% to 25% and 80% to 69%, respectively. It can also be observed from Figure 1C that the cell with mango dye had the highest absorption coefficient while the cell without dye had the lowest. After 1032 hours the absorption coefficients of pristine and device with cashew dye increased, this suggests better optical stability. As seen in Figure 1D, the reflectance of all samples is observed to reduce as we move from the UV to the NIR. After 1032 hours, samples containing dyes showed lesser reflectance compared to pristine, this further suggests that cashew and mango dyes could also be used in fabricating window layers in solar cells [37,49].

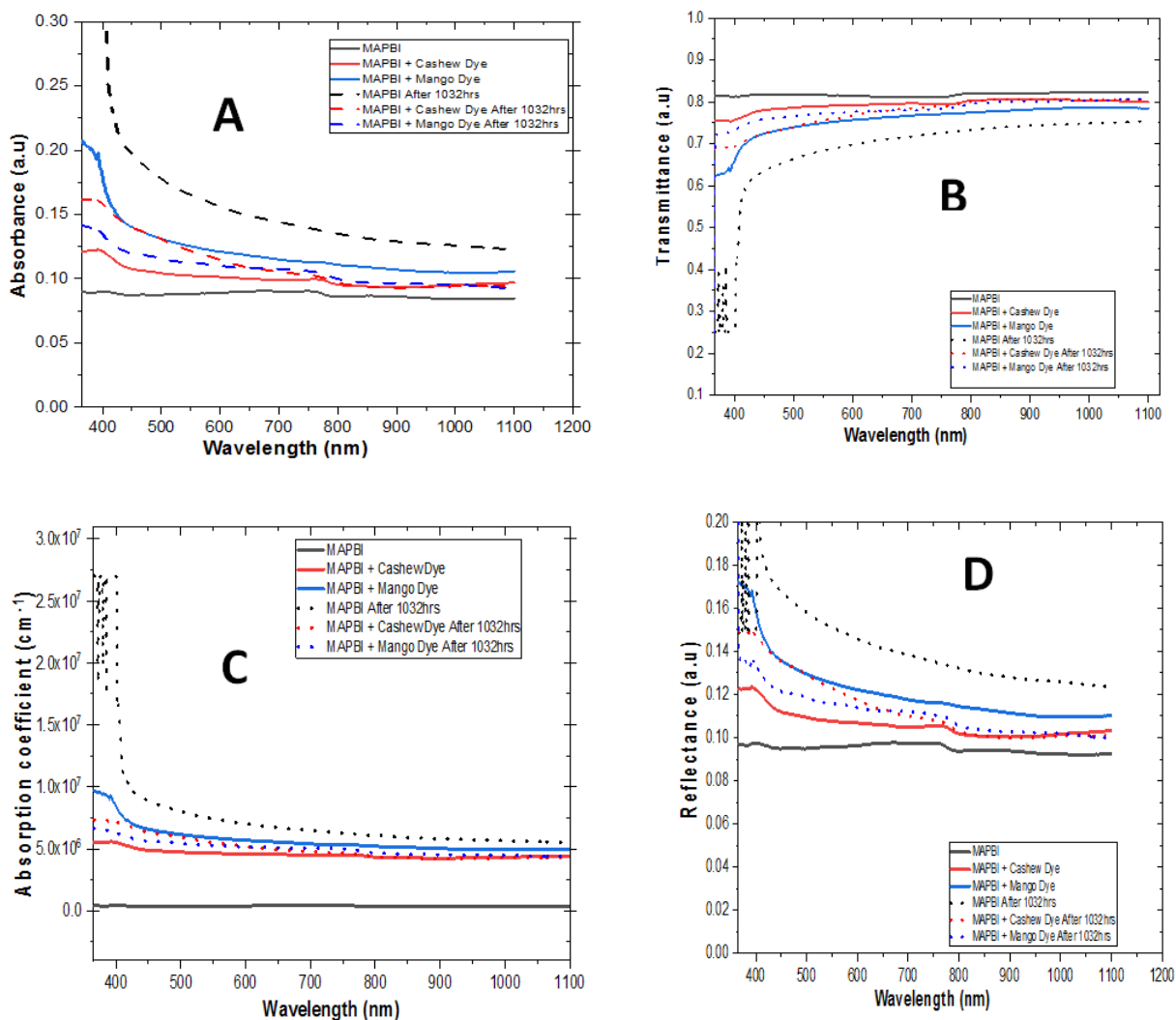


Figure 1. (A) Absorbance, (B) transmittance, (C) absorption coefficient, and (D) reflectance.

Energy Band Gap

Using the Tauc method for estimating bandgap, the intercept on the energy (eV) axis of the plot of $(\alpha h\nu)^2$ against photon energy indicates the optical band gap. The band gaps obtained were 1.59 eV, 1.70 eV, and 2.52 eV for pristine, Cashew dye cell, and Mango dye cell, respectively, as seen in Figure 2(A-C). These values are comparable with those reported in literature [11-15]. The modifications in the band gaps of these materials are attributed to the effect of cashew and mango

dyes. This result shows that cashew and mango dyes could be used in creating wide-band gap perovskite solar cells [31]. Figure 2(D-F) shows that after 1032 hours, the following band gaps 2.90 eV, 2.15 eV, 2.17 eV, for pristine, Cashew dye cell, and Mango dye cell, respectively. This suggests that the dye-treated samples had an improved optical band gap compared to the untreated even after 1032 hours. Band gaps for the fabricated cells is summarized in Table 1.

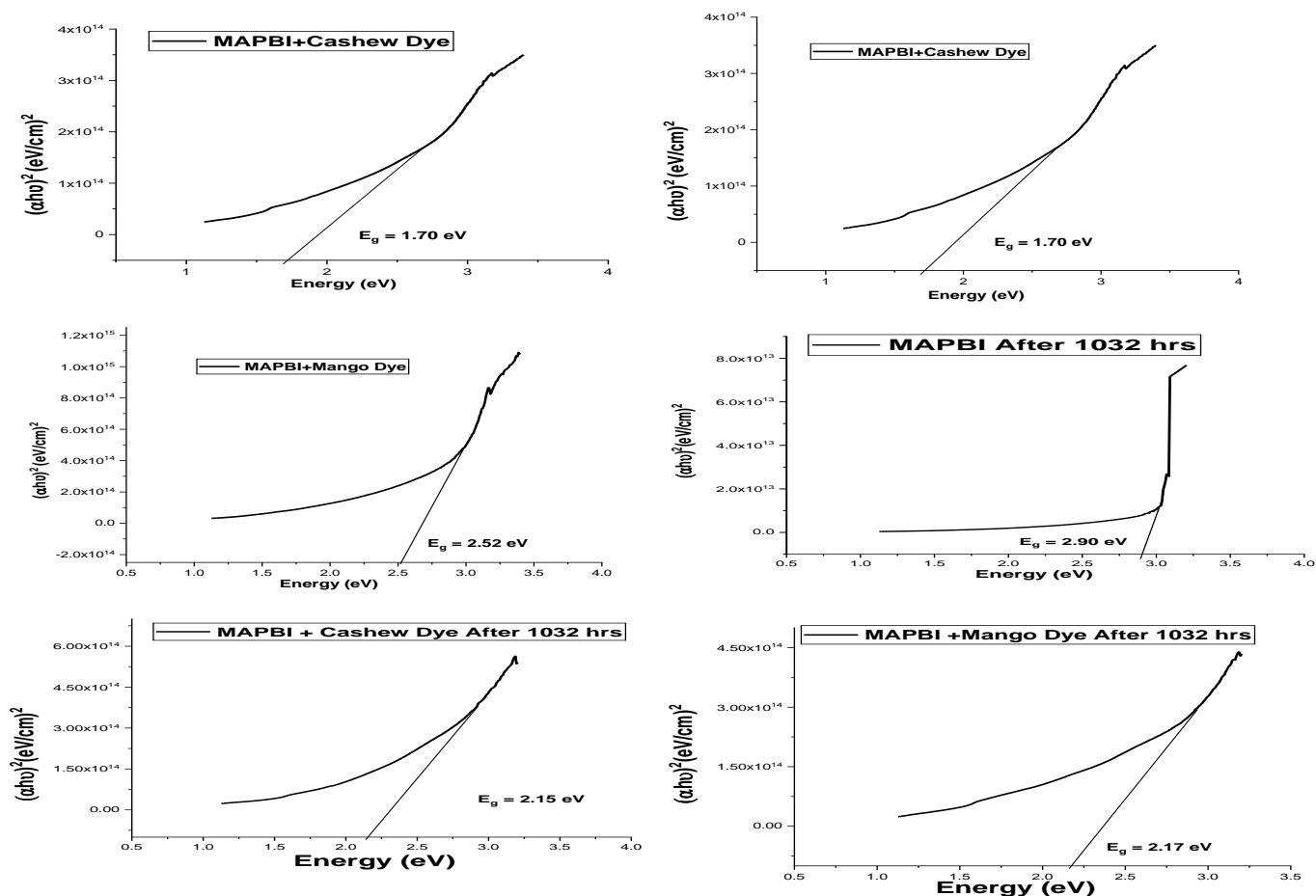


Figure 2. Energy bandgap of A-MAPBI, B-MAPBI+CASHW DYE, MAPBI+MANGO DYE, D-MAPBI after 1032hrs, E-MAPBI+CASHW after 1032 h, and F-MAPBI+MANGO after 1032 h.

Table 1. Summary of band gaps of samples

Sample	Band gap (eV)	Sample	Band gap (eV) after 1032 hours
Sample A	1.59	Sample D	2.90
Sample B	1.70	Sample E	2.15
Sample C	2.52	Sample F	2.17

Morphological Analysis of Samples

The morphological (surface features) properties of the synthesized pristine MAPbI₃ and those with different the selected plant dyes were studied using a scanning electron microscope (SEM), as demonstrated in Figure 3. The SEM image of pristine cell reveals the formation of fine cubic nanoparticles. In addition, surface pinholes, groves, and cracks caused by

degradation and mechanical stress due to the rapid thermal crystal growth can be seen in some sections of the image; these are evidence of defect and trap sites which cause charge recombination. The distinctive “shell-like” surface morphology observed in cell incorporated with Cashew dye as a result of agglomeration of nanoparticles at the grain boundaries made of crystals with different orientation and large sizes as confirmed in the

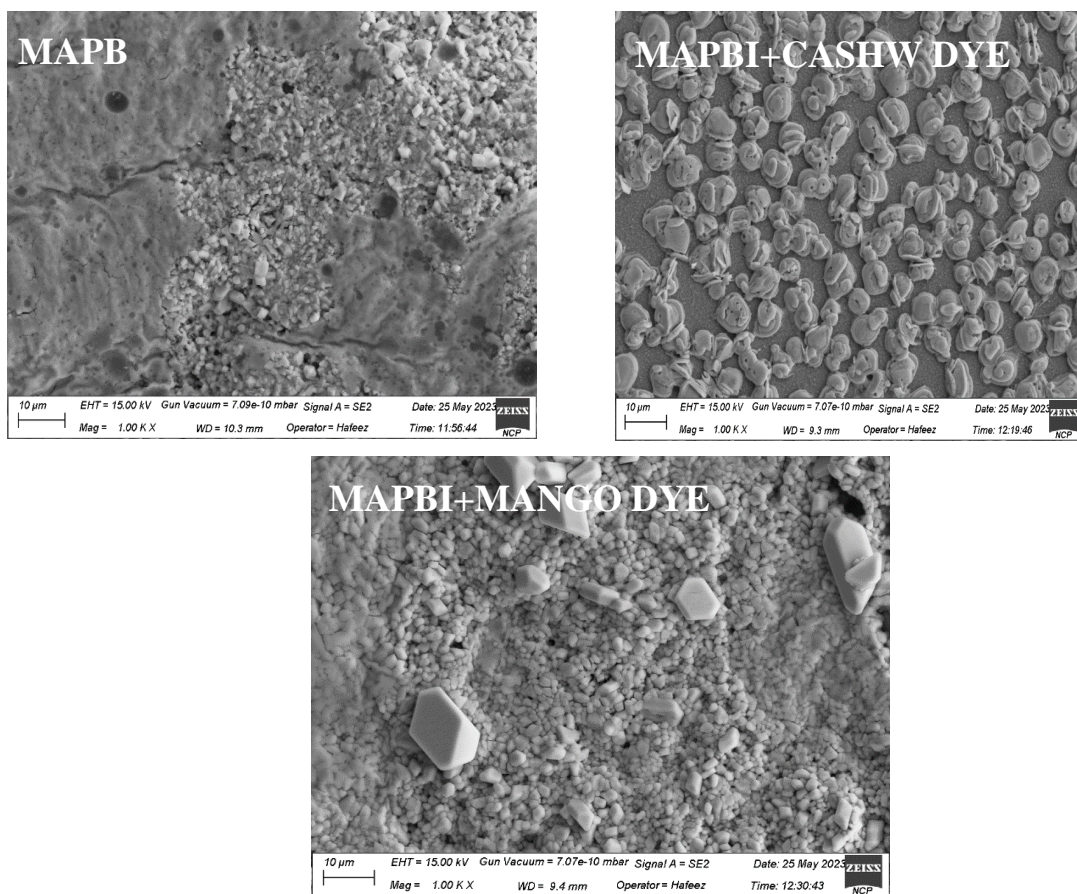


Figure 3. SEM of the perovskite solar cells.

XRD analysis. These boundaries which could indicate the transition between different crystalline orientations are suspected to be caused by the presence of the chemical elements in Cashew leaf dye, which affected the dynamics of the crystal growth of the film. According to Qiao *et al.* (2017), these nano shell-like core structures are reported to provide water-resistant barrier and long-term stability in perovskite [48]. The surface SEM image of cell with mango dye shows fine, uniform, and compact formation of cubic nanoparticles with minimal pore size and crack. This shows less mechanical stress and good crystal growth and coverage.

Elemental Analysis of EDX/EDS

Figure 4 presents the outcomes of Energy Dispersive X-ray Spectroscopy (EDX or EDS)

analysis, which has been instrumental in corroborating the elemental composition of the $\text{CH}_3\text{NH}_3\text{PbI}_3$ perovskite material deposited onto the glass substrate. The discerned EDX spectra reveal distinct peaks corresponding to all constituent elements expected within the $\text{CH}_3\text{NH}_3\text{PbI}_3$ perovskite structure, providing robust confirmation of the material's chemical makeup. Moreover, it is noteworthy that supplementary peaks have surfaced in the spectra, primarily attributable to the substrate material, which, in this case, is a Fluorine-doped Tin Oxide (FTO) glass. The conspicuous presence of silicon (Si) and Tin (Sn) peaks can be ascribed to the inherent composition of the FTO substrate, underscoring the sensitivity and reliability of the EDX technique in delineating material interfaces. Furthermore, an intriguing oxygen (O) peak has

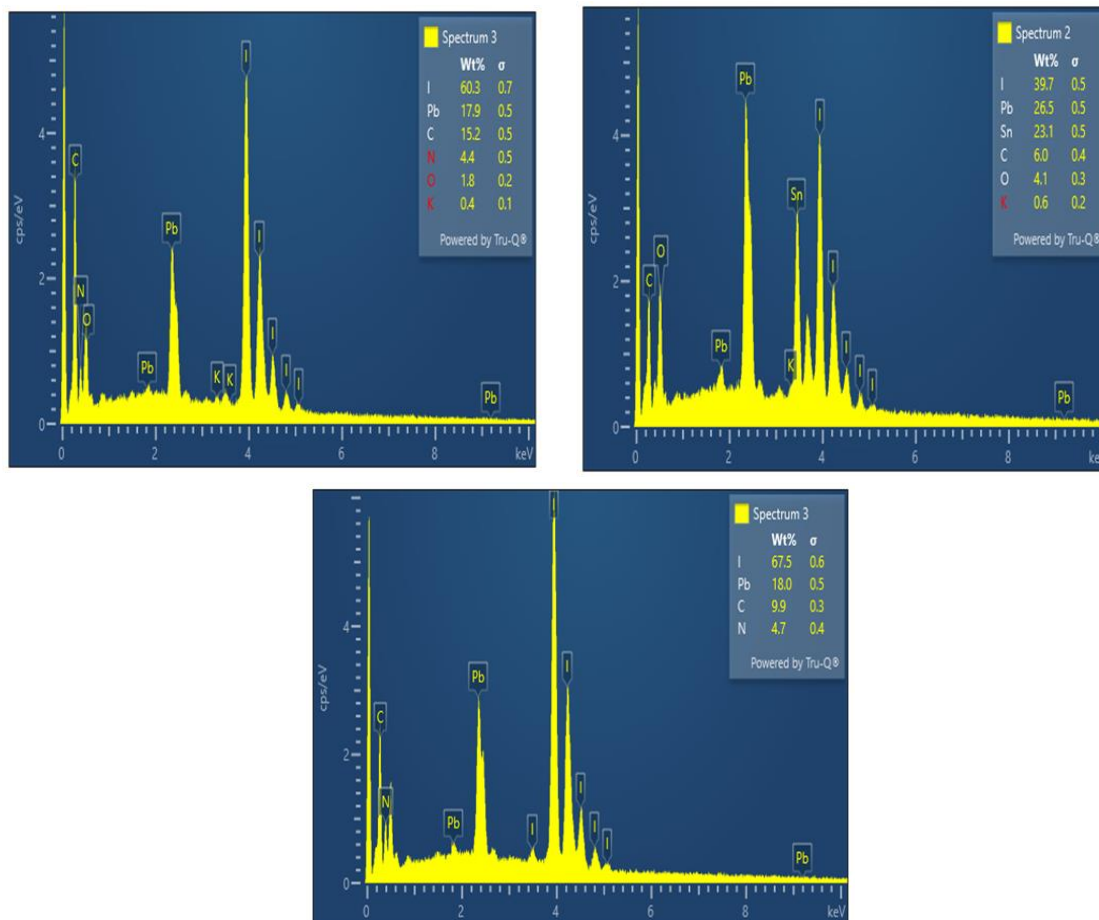


Figure 4. EDXs spectrum of perovskite solar cells.

been detected in the spectrum, which raises pertinent questions regarding its origin. Based on careful consideration, it is posited that this oxygen signal emanates from the interaction of the sample with the surrounding atmospheric conditions. This observation underscores the susceptibility of the perovskite material to oxidation upon exposure to the ambient atmosphere, an aspect that warrants further investigation and control in experimental setups.

XRD Analysis

The XRD maximum peaks of the prepared pristine MAPBI₃ were observed at a 2 θ value of 24.98° other peaks, as seen in Figure 5; correspond to 37.57°, 47.70°, 53.74° and 54.96°. The average crystallite size was calculated as

12.90 nm using Debye-Scherer's formula. The maximum XRD peak of MAPBI₃+CASHEW was observed at 2 θ values of 25.22°, other peaks are observed at 37.70°, 47.88°, 57.91°, and 62.67°. The average crystallite size was calculated as 15.01 nm. The maximum XRD peak of MAPBI₃+MANGO and dye was observed at 2 θ values of 25.08°, other peaks are observed at 37.70°, 47.67°, 53.59°, and 62.54°. The average crystallite size was calculated as 11.93 nm.

The XRD peaks confirm the polycrystalline nature of the fabricated solar cells. The untreated sample provides us with a baseline for comparison. The dislocation density and lattice strain in this sample are relatively low, indicating a well-structured crystal lattice. The crystal size is larger compared to the pristine sample, suggesting some agglomeration of nanoparticles.

This could be attributed to factors like sample preparation or natural variations in crystal growth. The optical absorption profile (Figure 1A) of the pristine sample shows moderate light absorption. Sample with cashew dye, exhibits several notable features. It has the lowest dislocation density and lattice strain among the samples, showing an improved crystal structure for the cashew dye compared to the pristine sample. The larger crystal size, as well as the presence of agglomerated nanoparticles observed in SEM (Figure 3), is suggested to contribute to crystal growth and stabilization. Likewise, since a larger crystal size improves absorption and charge transfer as well as reduces trap sites, the introduction of the cashew dye improves the optical absorption of the solar cell,

as seen in the absorption profiles (Figure 1A). The PSC with mango dye presents distinct characteristics compared to the other samples. It raises concerns due to its extremely high dislocation density and lattice strain, suggesting structural imperfections.

Photoelectric Conversion Analysis Using Solar Simulator

The photovoltaic parameters for the Perovskite Solar Cell (PSC) devices were determined under incident illumination with intensity of 920 mW/cm^2 using a cell area of 2.25 cm^2 . Figures 6 (A-C) illustrate the J-V curves corresponding to the PSC devices, while Table 3 presents a summary of the J-V parameters acquired. Both PSCs, which incorporated natural dye extracts

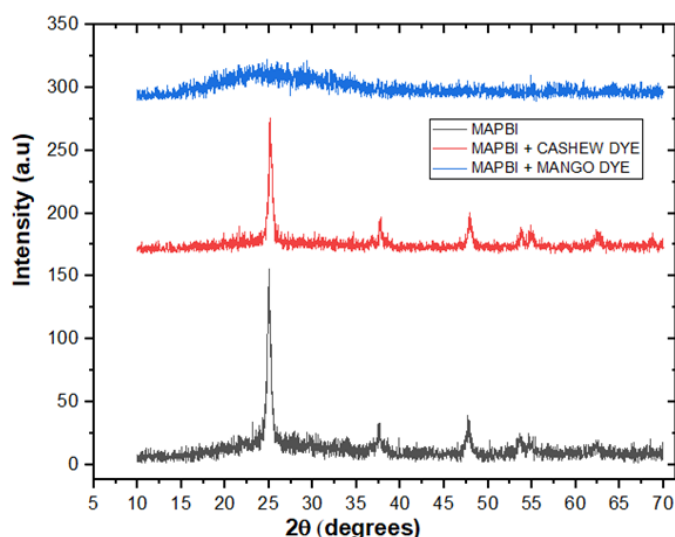


Figure 5. XRD plot of Perovskite solar cells.

Table 2. Summary of crystal parameters of the deposited perovskite samples

Samples	Angles 2θ (Degrees)	FWHM (β)	Crystal size, D (nm)	Inter-planar spacing, d(nm)	Dislocation density, $\delta(\text{nm}^{-2})$	Lattice strain, ϵ	Thickness of film (nm)
MAPBI	24.99	0.0113	12.9	0.026	0.006	0.013	222.11
MAPBI+Cashew Dye	25.16	0.0102	14.2	0.354	0.004	0.012	220.35
MAPBI+Mango Dye	25.88	0.2260	0.7	0.344	2.367	0.246	212.91

derived from cashew and mango sources, exhibit a reduction in the short-circuit current density (J_{sc}) when compared to the pristine PSC. This observation implies that the integration of natural dyes has an influence on the current generation capacity of the devices. Conversely, the open-circuit voltage (V_{oc}) remains relatively consistent across all three scenarios, suggesting that the presence of natural dye extracts does not significantly alter the voltage potential of the PSCs. Notably, the PSC incorporating mango dye extract demonstrates a significantly enhanced fill

factor (0.571) in comparison to both the pristine device (0.496) and the one with cashew dye extract (0.488). This improvement implies that the mango dye has potential of improving charge extraction and collection, thereby enhancing the overall performance of the device. Although the PSCs incorporating dye extracts exhibit lower Power Conversion Efficiency (PCE) values when contrasted with the pristine PSC, it is noteworthy that the PSC with mango dye extract yields a slightly higher PCE (0.0297%) compared to the PSC with cashew dye extract (0.0285%).

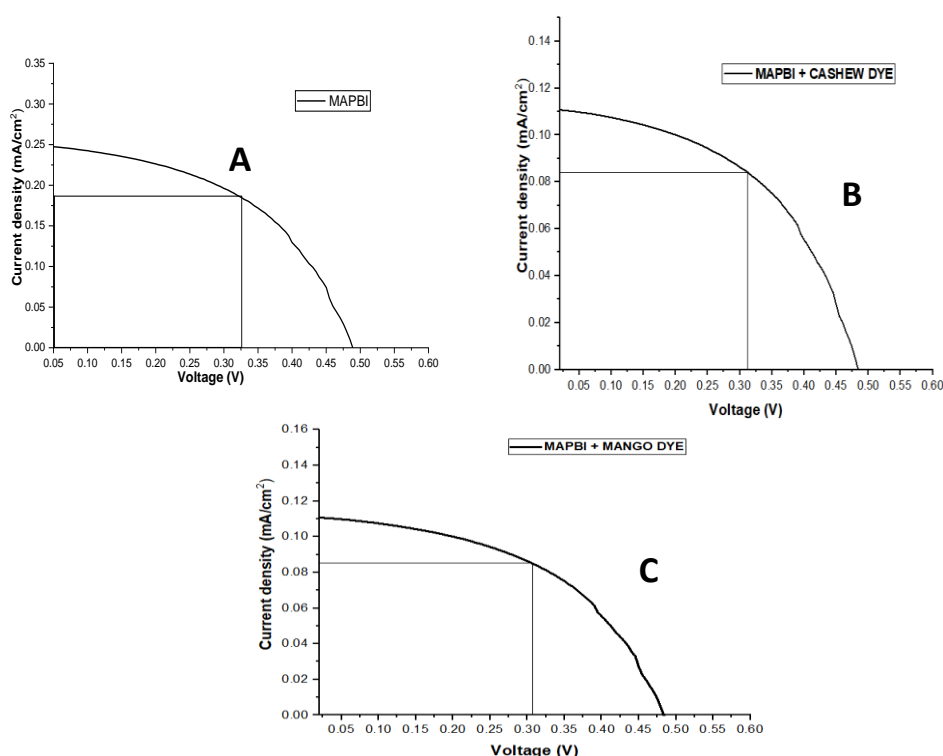


Figure 6. (A) MAPBI, (B) MAPBI-Cashew, and (C) MAPBI+MANGO JV plots of Perovskite solar cells.

Table 3. Summary of solar simulation parameters for all samples

Sample	J_{sc} (mA/cm ²)	J_m (mA/cm ²)	V_{oc} (V)	V_m (V)	FF	P_{max} (W/m ²)	Efficiency η %
MAPBI	0.250	0.186	0.488	0.325	0.496	0.605	0.0658
MAPBI+Cashew Dye	0.111	0.084	0.484	0.312	0.488	0.262	0.0285
MAPBI+Mango Dye	0.110	0.089	0.484	0.307	0.571	0.273	0.0297

Conclusion

In conclusion, the incorporation of natural dyes from cashew leaves and mango leaves in low-cost

inorganic methyl ammonium lead iodide ($CH_3NH_3PbI_3$) perovskite solar cells showed promising improvements in the optical

properties, crystal structure, and stability. The dye-treated devices exhibited enhanced absorbance, transmittance, and band gap values compared to the pristine device. The performance and stability evaluation of a low-cost inorganic methyl Ammonium lead iodide ($\text{CH}_3\text{NH}_3\text{PbI}_3$) perovskite solar cells enhanced with natural dyes from Cashew leaves and Mango leaves were done through optical characterization, XRD, SEM, EDX, and solar simulation of the prepared perovskite solar cells. The band gap of the materials was obtained as 1.59 eV, 1.70 eV, and 2.52 eV for pristine, cashew dye, and mango dye incorporated devices respectively. The peaks obtained from the XRD studies confirm that the samples prepared are polycrystalline. The addition of cashew dye, demonstrates the most promising characteristics among the three samples. It exhibits an improved crystal structure, larger crystal size, enhanced light absorption, reduced trap sites, and improved stability. These findings emphasize the potential of cashew dye additive for high-performance perovskite solar cells. The pristine sample, serves as a valuable reference point, while the structural imperfections shown in the PSC containing mango dye extract highlights the need for further research and optimization efforts in this direction to warrant the maximization its potential. The pristine PSC device's maximum power conversion efficiency (PCE) was found to be 0.0658%. Comparatively, the device containing mango dye had a PCE of 0.0297%. with an improved fill factor (FF) of 0.571 compared to the pristine device (FF = 0.496), suggesting the potential influence of the incorporated dye derived from cashew leaves. The stability of the prepared samples was evaluated by studying their optical properties after exposure under room temperature and conditions for 1032 hours.

Authors' Contribution

Ejeka Joshua Chukwuemeka, Udeze Chinwe Uchechukwu, and Imosobomeh L. Ikhioya: Conceptualization, Methodology, and Original Draft Writing. Anyanor Oliver Odira and Jeroh, Diemiruaye Mimi: Software and editing. Imosobomeh L. Ikhioya and Nwokoye Anthony Osita: Investigation and visualization.

Conflict of interest

The authors affirm no financial or interpersonal conflicts affected the research in this study.

Data availability

Data can be given upon request.

Orcid

Ejeka J. Chukwuemeka : [0009-0005-5885-5073](https://orcid.org/0009-0005-5885-5073)

Udeze C. Uchechukwu : [0009-0009-1666-0568](https://orcid.org/0009-0009-1666-0568)

Jeroh D. Mimi : [0000-0002-1622-0337](https://orcid.org/0000-0002-1622-0337)

Imosobomeh L. Ikhioya : [0000-0002-5959-4427](https://orcid.org/0000-0002-5959-4427)

References

- [1] A. Nwokoye, *Solar Energy Technology: Other Alternative Energy Resources and Environmental Science*, Rex Charles and Patrick Publications: Nigeria, **2010**, pp. 234–243.
- [2] L.E. Erickson, *Environ. Prog. Sustain. Energy.*, **2017**, *36*, 982–988. [[CrossRef](#)], [[Google Scholar](#)], [[Publisher](#)]
- [3] A.O. Akankpo, A. Adeniran, F. Ayedun, O. Anyanor, G. Ebong. *J. Res. Environ. Earth Sci.*, **2023**, *9*, 57–63. [[Google Scholar](#)]
- [4] I. Onyeka Anthony, E. Joshua C, A. Oliver O, *Phys. Sci. Int. J.*, **2021**, *25*, 1–7. [[CrossRef](#)], [[Google Scholar](#)]
- [5] O. Anyanor, A. Nwokoye, O. Ikenga, C. Emergonu, *J. Eng. Res. Rep.*, **2021**, *20*, 115–127. [[Google Scholar](#)]
- [6] M. Green, E. Dunlop, J. Hohl-Ebinger, M. Yoshita, N. Kopidakis, X. Hao, *Prog.*

- Photovoltaics Res. Appl.*, **2021**, *29*, 3–15. [CrossRef], [Google Scholar], [Publisher]
- [7] J.P. Correa-Baena, A. Abate, M. Saliba, W. Tress, T.J. Jacobsson, M. Grätzel, A. Hagfeldt, *Energy Environ. Sci.*, **2017**, *10*, 710–727. [CrossRef], [Google Scholar], [Publisher]
- [8] A. Kojima, K. Teshima, Y. Shirai, T. Miyasaka, *J. Am. Chem. Soc.*, **2009**, *131*, 6050–6051. [CrossRef], [Google Scholar], [Publisher]
- [9] A.M. Elseman, D.W. Sajid, A.E. Shalan, M.M. Rashad, M. Li, *Pathways towards high-stable, low-cost and efficient perovskite solar cells*, **2018**, p. 201. [CrossRef], [Google Scholar], [Publisher]
- [10] R.D. Chavan, D. Prochowicz, M.M. Tavakoli, P. Yadav, C.K. Hong, *Adv. Mater. Interfaces.*, **2020**, *7*, 2000105. [CrossRef], [Google Scholar], [Publisher]
- [11] W. Chen, Y. Zhu, J. Xiu, G. Chen, H. Liang, S. Liu, H. Xue, E. Birgersson, J.W. Ho, X. Qin, *Nat. Energy.*, **2022**, *7*, 229–237. [CrossRef], [Google Scholar], [Publisher]
- [12] Y. Qi, D. Ndaleh, W.E. Meador, J.H. Delcamp, G. Hill, N.R. Pradhan, Q. Dai, *ACS Appl. Energy Mater.*, **2021**, *4*, 9525–9533. [CrossRef], [Google Scholar], [Publisher]
- [13] A. Mahapatra, D. Prochowicz, M.M. Tavakoli, S. Trivedi, P. Kumar, P. Yadav, *J. Mater. Chem. A.*, **2020**, *8*, 27–54. [CrossRef], [Google Scholar], [Publisher]
- [14] S. Wang, Z. He, J. Yang, T. Li, X. Pu, J. Han, Q. Cao, B. Gao, X. Li, *J. Energy Chem.*, **2021**, *60*, 169–177. [CrossRef], [Google Scholar], [Publisher]
- [15] M. Hosseinneshad, *J. Electron. Mater.*, **2019**, *48*, 5403–5408. [CrossRef], [Google Scholar], [Publisher]
- [16] J. Bisquert, E.J. Juarez-Perez, *Phys. Chem. Lett.*, **2019**, *10*, 5889–5891. [CrossRef], [Google Scholar], [Publisher]
- [17] A.C. Nkele, A.C. Nwanya, N.U. Nwankwo, R.U. Osuji, A. Ekwealor, P.M. Ejikeme, M. Maaza, F.I. Ezema, *Adv. Nat. Sci.: Nanosci. Nanotechnol.*, **2019**, *10*, 045009. [CrossRef], [Google Scholar], [Publisher]
- [18] X. He, J. Chen, X. Ren, L. Zhang, Y. Liu, J. Feng, J. Fang, K. Zhao, S. Liu, *Adv. Mater.*, **2021**, *33*, 2100770. [CrossRef], [Google Scholar], [Publisher]
- [19] Sk. Salauddin, M. Anamul, S. Al Mojnun, *Text. Leather Rev.*, **2021**, *4*, 218–233. [CrossRef], [Google Scholar], [Publisher]
- [20] X. Kong, L. Hou, Y. Qian, H. Wang, Z. Xu, *ICOMD 2021.*, **2022**, *12164*, 150–154. [CrossRef], [Google Scholar], [Publisher]
- [21] U. Uno, M. Emeteri, L. Fadipe, J. Oyediji, *Int. J. Appl. Eng. Res.*, **2015**, *10*, 17685–17695. [Google Scholar], [Publisher]
- [22] S. Vaithilingam, K. Jayanthi, A. Muthukaruppan, *Polymer*, **2017**, *108*, 449–461. [CrossRef], [Google Scholar], [Publisher]
- [23] P.O. Isi, A.J. Ekpunobi, D.N. Okoli, (*IOSR-JAP*), **2021**, *13*, 01.
- [24] L.U. Okoli, J.O. Ozuomba, A.J. Ekpunobi, *Res. J. Physical Sci.*, **2013**, *4*, 6–10. [Google Scholar]
- [25] K.U. Isah, A.Y. Sadik, B.J. Jolayemi, *Eur. J. Appl. Sci.*, **2017**, *9*, 140–146 [CrossRef], [Google Scholar], [Publisher]
- [26] H. Setyawati, *Results Phys.*, **2017**, *7*, 2907–2918. [CrossRef], [Google Scholar], [Publisher]
- [27] M.A. Al-Alwani, A.B. Mohamad, A.A.H. Kadhum, N.A. Ludin, *Spectrochim. Acta A: Mol. Biomol. Spectrosc.*, **2015**, *138*, 130–137. [CrossRef], [Google Scholar], [Publisher]
- [28] E.C. Okafor, D.N. Okoli, I.L. Ikhioya, *Int. J. Appl. Phys.*, **2022**, *9*, 44. [CrossRef], [Google Scholar], [Publisher]
- [29] L. Jayamohan, V.S. Nair, *J. Phys. Conf. Ser.*, **2022**, *2357*, 012012. [CrossRef], [Google Scholar], [Publisher]
- [30] L.A. Ozobialu, A. J. Ekpunobi, D.M. Jeroh, *Int. J. Appl. Phys.*, **2021**, 2350–0301. [CrossRef], [Google Scholar], [Publisher]
- [31] A. Gürses, M. Açıkıldız, K. Güneş, M.S. Gürses, M. Açıkıldız, K. Güneş, M.S. Gürses, *Classification of Dye and Pigments*, Springer,

- 2016, pp. 31–45. [[CrossRef](#)], [[Google Scholar](#)], [[Publisher](#)]
- [32] F. Ghanaat, L. Vafajoo, M. Haddadi, *Prog. Chem. Biochem. Res.*, **2022**, 5, 331–337. [[CrossRef](#)], [[Google Scholar](#)], [[Publisher](#)]
- [33] S. Vaithilingam, K.P. Jayanthi, A. Muthukaruppan, *Polymer*, **2017**, 108, 449–461. [[CrossRef](#)], [[Google Scholar](#)], [[Publisher](#)]
- [34] A.H. Tullo, *C&EN.*, **2008**, 86, 26–27. [[CrossRef](#)], [[Publisher](#)]
- [35] M.C. Guamán-Balcázar, A. Montes, C. Pereyra, E.M. de la Ossa, *J. Supercrit. Fluids.*, **2017**, 128, 218–226. [[CrossRef](#)], [[Google Scholar](#)], [[Publisher](#)]
- [36] I.F. Okoye, A.O.C. Nwokoye, G. Ahmad, *Energy Power Eng. Sci.*, **2021**, 13, 221–235. [[CrossRef](#)], [[Google Scholar](#)], [[Publisher](#)]
- [37] A.M. Hasan, I. Raifuku, N. Amin, Y. Ishikawa, D. Sarkar, K. Sobayel, M.R. Karim, A. Ul-Hamid, H. Abdullah, M. Shahiduzzaman, *Opt. Mater. Express.*, **2020**, 10, 1801–1816. [[CrossRef](#)], [[Google Scholar](#)], [[Publisher](#)]
- [38] P.K. Kung, M.H. Li, P.Y. Lin, Y.H. Chiang, C.R. Chan, T.F. Guo, P. Chen, *Adv. Mater. Interfaces*, **2018**, 5, 1800882. [[CrossRef](#)], [[Google Scholar](#)], [[Publisher](#)]
- [39] J.R. Manders, S.W. Tsang, M.J. Hartel, T.H. Lai, S. Chen, C.M. Amb, J.R. Reynolds, F. So, *Adv. Funct. Mater.*, **2013**, 23, 2993–3001. [[CrossRef](#)], [[Google Scholar](#)], [[Publisher](#)]
- [40] Q. He, K. Yao, X. Wang, X. Xia, S. Leng, F. Li, *ACS Appl. Mater. Interfaces.*, **2017**, 9, 41887–41897. [[CrossRef](#)], [[Google Scholar](#)], [[Publisher](#)]
- [41] A.A.S. Marques, R.M. Faria, J.N. Freitas, A.F. Nogueira, *Ind. Eng. Chem. Res.*, **2021**, 60, 7145–7154. [[CrossRef](#)], [[Google Scholar](#)], [[Publisher](#)]
- [42] I.L. Ikhioya, A.C. Nkele, D. Okoli, A. Ekpunobi, I. Ahmed, *J. Indian Chem. Soc.*, **2022**, 99, 100641. [[CrossRef](#)], [[Google Scholar](#)], [[Publisher](#)]
- [43] K.I. Udofia, I.L. Ikhioya, D.N. Okoli, Azubike J. Ekpunobi, *J. Med. Nanomater. Chem.*, **2023**, 5, 135–147. [[CrossRef](#)], [[Publisher](#)]
- [44] I.L. Ikhioya, I. Nwamaka, E.U. Akpu, Onoh, S.O. Aisida, I. Ahmad, M. Maaza, F.I. Ezema, *J. Med. Nanomater. Chem.*, **2023**, 6, 156–167. [[CrossRef](#)], [[Publisher](#)]
- [45] I. Rufus, A. Peter, S.O. Aisida, I.L. Ikhioya, *Results Opt.*, **2023**, 12, 100464. [[CrossRef](#)], [[Google Scholar](#)], [[Publisher](#)]
- [46] I.L. Ikhioya, S.O. Aisida, I. Ahmad, F.I. Ezema, *Chem. Phys. Impact*, **2023**, 7, 100269. [[CrossRef](#)], [[Google Scholar](#)], [[Publisher](#)]
- [47] Z. Ouyang, M. Yang, J.B. Whitaker, D. Li, M.F. van Hest, *ACS Appl. Energy Mater.*, **2020**, 3, 3714–3720. [[CrossRef](#)], [[Google Scholar](#)], [[Publisher](#)]
- [48] B. Qiao, P. Song, J. Cao, S. Zhao, Z. Shen, D. Gao, Z. Liang, Z. Xu, D. Song, X. Xu, *Nanotechnology*, **2017**, 28, 445602. [[CrossRef](#)], [[Google Scholar](#)], [[Publisher](#)]
- [49] I.L. Ikhioya, N.I. Akpu, A.C. Nkele, *Mater. Res. Express*, **2021**, 8, 016403. [[CrossRef](#)], [[Google Scholar](#)], [[Publisher](#)]

HOW TO CITE THIS ARTICLE

Ejeka Joshua Chukwuemeka, Nwokoye Anthony Osita, Anyanor Oliver Odira, Udeze Chinwe Uchechukwu, Jeroh Diemiruaye Mimi, Imosobomeh Lucky Ikhioya*. Performance and Stability Evaluation of Low-Cost Inorganic Methyl Ammonium Lead Iodide (CH₃NH₃PbI₃) Perovskite Solar Cells Enhanced with Natural Dyes from Cashew and Mango Leaves. *Adv. J. Chem. A*, 2024, 7(1), 21-40.

DOI: [10.48309/AJCA.2024.406961.1384](https://doi.org/10.48309/AJCA.2024.406961.1384)

URL: https://www.ajchem-a.com/article_181551.html